

<http://www.glaciology.ethz.ch>

ICEQUAKES COUPLED WITH SURFACE DISPLACEMENTS FOR PREDICTING GLACIER BREAK-OFF

J. FAILLETTAZ, D. SORNETTE, AND M. FUNK

ABSTRACT. A hanging glacier at the east face of Weisshorn (Switzerland) broke off in 2005. We were able to monitor and measure surface motion and icequake activity for 25 days up to three days prior to the break-off. The analysis of seismic waves generated by the glacier during the rupture maturation process revealed four types of precursory signals of the imminent catastrophic rupture: (i) an increase in seismic activity within the glacier, (ii) a decrease in the waiting time between two successive icequakes, (iii) a change in the size-frequency distribution of icequake energy, and (iv) a modification in the structure of the waiting time distributions between two successive icequakes. Moreover, it was possible to demonstrate the existence of a correlation between the seismic activity and the log-periodic oscillations of the surface velocities superimposed on the global acceleration of the glacier during the rupture maturation. Analysis of the seismic activity led us to the identification of two regimes: a stable phase with diffuse damage, and an unstable and dangerous phase characterized by a hierarchical cascade of rupture instabilities where large icequakes are triggered.

1. INTRODUCTION

The fracturing of brittle heterogeneous material has often been studied at the laboratory scale using acoustic emission measurements (see for instance Johansen and Sornette (2000); Nechad and others (2005a) for recent observations interpreted using concepts relevant to the present study). These studies reported an acceleration of brittle damage before failure. Acoustic emission tools have already been used at meso-scale to find precursors to natural gravity-driven instabilities such as cliff collapse (Amitrano and others, 2005) or slope instabilities (Dixon and Spriggs, 2007; Kolesnikov and others, 2003; Dixon and others, 2003). The present paper focuses on the acoustic emissions generated by an unstable glacier. To our knowledge, this is the first attempt to use these acoustic emissions to predict the catastrophic break-off of a glacier.

Ice mass break-off is a natural gravity-driven instability as found in the case of a landslide, rockfalls or mountain collapse. Such glacier break-off represents a considerable risk to mountain communities and transit facilities situated below, especially in winter, as an ice avalanche may drag snow in its train. In certain cases, an accurate prediction of this natural phenomenon is necessary in order to prevent such dangerous events. The first attempt to predict such break-offs was conducted in 1973 by Flotron (1977) and R othlisberger (1981) on the Weisshorn hanging glacier. This latter author measured the surface velocity of the unstable glacier and proposed an empirical function to fit the increasing surface velocities before break-off. This function describes an acceleration of the surface displacement

Key words and phrases. glacier, rupture, prediction, icequakes.

following a power law up to infinity at a finite time t_c . Obviously, the real break-off will necessarily occur before t_c , but the method gives a good description of the surface velocity evolution until rupture. Recently, following Lüthi (2003) and Pralong and others (2005), Faillettaz and others (2008) showed evidence of an oscillatory behaviour superimposed on the general acceleration which enables a more accurate determination of the time of rupture. Faillettaz and others (2008) showed also an increase in icequake activity before the break-off. The aim of this paper is to present (i) a careful analysis of these seismic measurements, (ii) our conclusions in terms of rupture processes, and (iii) perspectives for forecasting.

Several studies have shown that glaciers can generate seismic signals called icequakes. Previous studies have identified at least five characteristic seismic waveforms associated with five different icequake event types. These include: 1) surface crevassing (high frequency, short duration, impulsive onsets, Neave and Savage (1970); Deichmann and others (2000); Walter and others (2008)), 2) calving events (Low frequency, long duration, non-impulsive onsets, surface waves, O'Neel and others (2007); Neetles and others (2008)), 3) basal sliding (low frequency, short duration, no surface waves, Weaver and Malone (1979)) 4) iceberg interaction (low frequency, long duration, multiple harmonic frequencies, MacAyeal and others (2008)), and 5) hydraulic transients in glacial water channels (low frequency, emergent onset, absence of distinct S wave, St Lawrence and Qamar (1979)).

In this study, the focus is on seismic activity generated by a cold hanging glacier before its break-off. The crucial features of this type of glacier are as follows: (i) there is no sliding at the bedrock, and (ii) the glacier is entirely cold and there is no water within the ice. Precursory seismic signals were detected, and a change in the behavior occurred two weeks before the global rupture.

2. WEISSHORN GLACIER AND THE HISTORY OF EVENTS

The northeast face of the Weisshorn (Valais, Switzerland) is covered with unbalanced cold ramp glaciers (i.e., the snow accumulation is, for the most part, compensated by break-off, Pralong and Funk, 2006), located between 4500 m and 3800 m a.s.l., on a steep slope of 45 to 50 degrees. In winter, snow avalanches triggered by icefalls pose a recurrent threat to the 400 inhabitants of the village of Randa located some 2500 m below the glacier, and to transit routes to Zermatt (see Fig. 1) (Raymond and others, 2003). In a compilation of historical records, Raymond and others (2003) showed that, despite no seasonal pattern in the events, Randa was damaged repeatedly during the last centuries, always in winter. Among the 19 events recorded since 1636, three caused a total of 51 fatalities, and six damaged the village of Randa. The Weisshorn hanging glacier broke off five times in the last 35 years (1973, 1980, 1986, 1999 and 2005, see Raymond and others (2003)); two of these events (in 1973 and 2005) were monitored in detail (Flotron, 1977; Faillettaz and others, 2008).

The total volume of the unstable ice mass was estimated at $0.5 \times 10^6 \text{ m}^3$ by means of photogrammetry (Faillettaz and others, 2008). Because of the dangerous situation for the village of Randa, a monitoring system was installed to alert the population of an impending break-off.

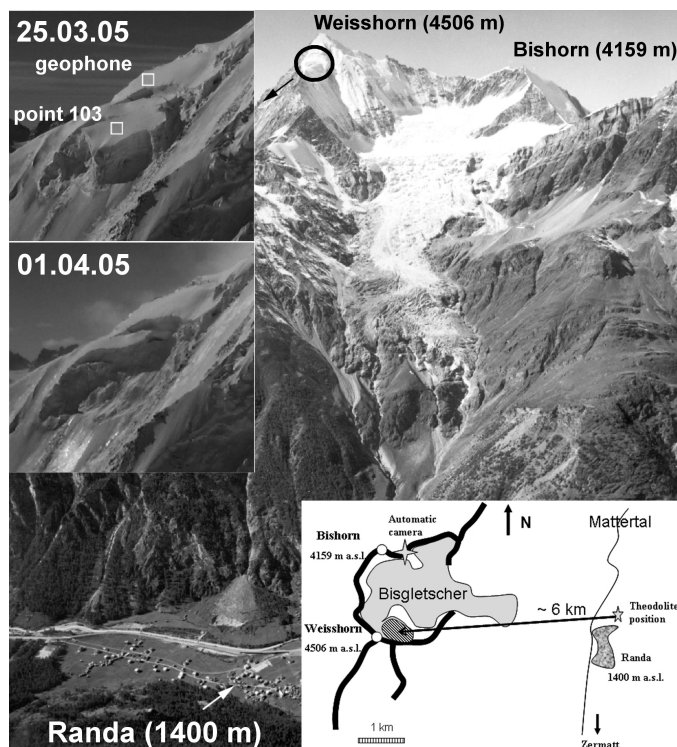


FIGURE 1. The east face of Weissshorn with the hanging glacier. The village of Randa and transit routes are visible in the valley. The ellipse indicates the location of the hanging glacier. The left insets show a closer frontal view of the hanging glacier on March, 25th 2005 before the second break-off (upper), and on April 1st, 2005 after the break-off (lower), including the positions of the geophone and stake 103 used for displacement measurements. The bottom right inset gives a general schematic view of the Weissshorn hanging glacier (dashed zone), and the monitoring setting (theodolite and automatic camera). Thick black lines indicate the mountain ridges, and the thin line represents the bottom of the valley.

3. METHODS

3.1. Instrumentation. An automatic camera (installed in September 2003 on the Bishorn, see Fig. 1) provided a detailed movie of the destabilization of the glacier. A first break-off occurred on March 24, 2005 (after 26.5 days of monitoring). Its estimated volume amounted to $120,000 \text{ m}^3$ (comparable to the 1973 break-off with $160,000 \text{ m}^3$). On March 31, 2005, a second rupture occurred, during which the major part of the glacier broke off (after 33.5 days of monitoring). The volume of this second ice avalanche was estimated at $400,000 \text{ m}^3$.

A single geophone (Lennartz LE-3Dlite Mkl, 3 orthogonal sensors, with eigenfrequency of 1 Hz) was installed in firn 30 cm below the surface near the upper

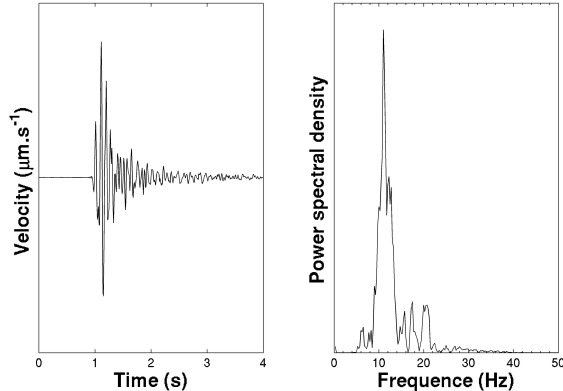


FIGURE 2. Unfiltered velocity seismogram of a typical event (maximum amplitude $2.5 \mu\text{m}\cdot\text{s}^{-1}$) and its corresponding normalized power spectrum density (right).

crevasse (Fig. 1), in order to record icequake activity before the final rupture. This signal is assumed to describe the crack (or damage) evolution within the ice mass during the failure process. A Taurus portable seismograph (Nanometrics inc.) was used to record the seismic activity of the glacier prior to its rupture with a sampling rate of 100 Hz. Unfortunately, the recorder failed on March 21, before the first break-off event, because of battery problems. A first seismic analysis of these measurements was presented in Faillettaz and others (2008).

Concurrently to the seismic measurements, we performed a careful analysis of the surface displacements of the glacier (see Fig. 3). The measurement equipment consisted of a total station (Leica theodolite TM1800 combined with the DI3000S Distometer) installed at a fixed position above Randa on the other side of the valley, and seven reflectors mounted on stakes drilled into the unstable ice mass. A reference reflector was installed on a rock for the correction of the measurements, because of broad variations in meteorological conditions. This fully autonomous apparatus performed the measurements every two hours. The motion of the reflectors (see Fig. 1) could be monitored only when the visibility conditions were good enough.

3.2. Analytical methods.

Icequake detection. We identified seismic events both visually and by using an automatic earthquake detection method based on the ratio of the root-mean-square between the short-term average (STA) window and the long-term average (LTA) window. The detection of events was performed in the following way. First, we evaluated the root-mean-square (rms) of two concurrent time windows. The rms values over the previous 800 ms long-term average (LTA) window and the previous 80 ms short-term average (STA) window were calculated and compared. When the ratio $\gamma = \text{STA}/\text{LTA}$ exceeded a given threshold (taken here equal to 3), an event was detected and retained (Allen, 1978; Walter and others, 2008). Both of these catalogues (with visual and automated detection) are compatible with each other

and give a total number of 1731 icequakes during the monitoring period (see Fig. 3).

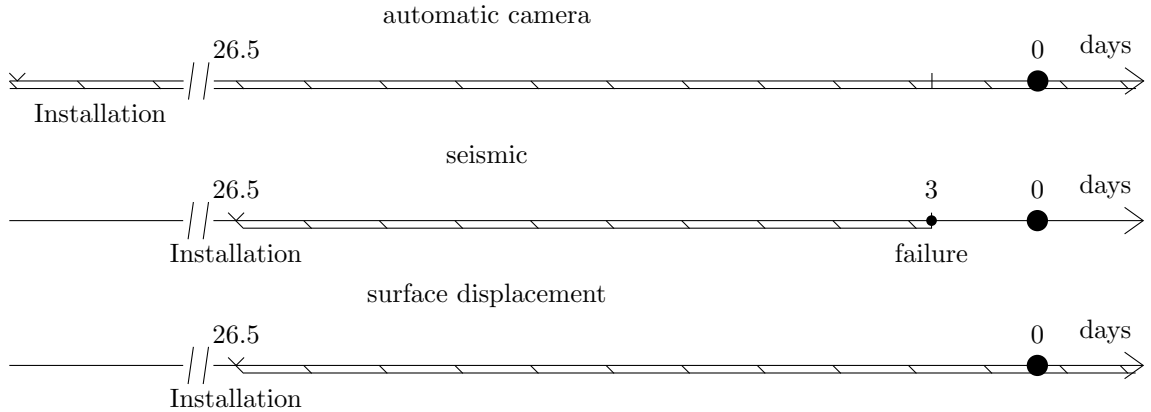


FIGURE 3. Timeline of monitoring. The origin of time 0 corresponds to the occurrence of the first break-off on March 24, 2005 (after 26.5 days of monitoring) with an estimated volume of about 120,000 m³.

Icequake characterization. For a much deeper analysis and to allow a comparison of the detected icequakes, their sizes were first evaluated. Seismic event sizes were estimated based on their signal energies as defined for a digitalized signal by Amitrano and others (2005):

$$(3.1) \quad E = \sum A^2 \delta t ,$$

where A is the signal amplitude and δt is the sampling period. We made a manual selection of the beginning and the end of each of the 1731 signals and performed the discrete summation for the evaluated duration of each event.

Finally, these methods enabled a catalogue of events to be obtained, containing time of occurrence and the respective energy for each detected icequake. It was then possible to analyse this catalogue with statistical tools and methods developed for earthquake study.

4. RESULTS

4.1. Signal characteristics. The data show a high seismic emissivity from the hanging glacier during the time span of our observations. In the case of the Weisshorn hanging glacier, seismic events with short and impulsive signals and similar spectra were observed (see Fig. 2), with dominant power contained in the 10-30 Hz frequency band. This observation is consistent with previous results (Neave and Savage, 1970; Deichmann and others, 2000; Roux and others, 2008; O’Neel and others, 2007).

This result is not surprising, as no serac falls could be observed during the time span of our observations (based on daily photographs). Since the sensor was very close to the sources, attenuation was low. The proximity of the source (less than 300 meters) gave rise to difficulties in distinguishing P and S waves.

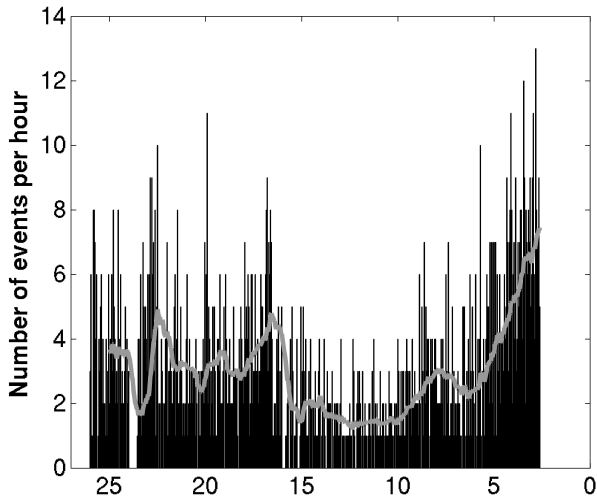


FIGURE 4. Number of detected icequakes per hour (bars in black) as a function of time shown on the abscissa. The smoothed number of icequakes per hour, shown as the light grey line, was obtained by averaging in a sliding window of 24 hours.

As the geophone was situated above the upper crevasse separating the active from the stable zone, compressive seismic waves (primary wave) were perturbed by the discontinuity of the material and therefore were less likely to be observed.

Figure 4 shows the number of detected events per hour during the 25-day period of the ice chunk destabilization. An acceleration of the seismic activity was detected one week before the first break-off (i.e., two weeks before the main break-off).

4.2. Size-frequency distribution of icequake energies. The complementary cumulative size-frequency (also called “survival”) distribution (CSFD) of the icequake energy preceding the break-off was then determined. The complementary Cumulative Distribution Function denotes the probability that the variable takes a value greater than x . In our case, the CSFD indicates the probability that the energy of an icequake will take a value greater than a given value.

In order to study the temporal variation of the CSFD, we used a moving window of 200 events with a 20-event shift between successive windows. We analyzed the event size distribution corresponding to each window (Fig. 5, top, shows three typical windows). The exponent β (Fig. 5, bottom) was estimated using the Maximum-Likelihood fitting method with goodness-of-fit tests based on the Smirnov test (often improperly known as the Kolmogorov-Smirnov test) (see for instance Clauset and others (2009) for a review on practical issues and empirical analyses). For each exponent, we used a goodness-of-fit test, which generates a p-value that quantifies the plausibility of the power law hypothesis. The purpose of this test is to sample many synthetic data sets from a true power-law distribution and to measure how far they fluctuate away from the power law form, and to compare the results with similar measurements of the empirical data. The quantification of the distance between two distributions was made using the Kolmogorov-Smirnov statistics. The

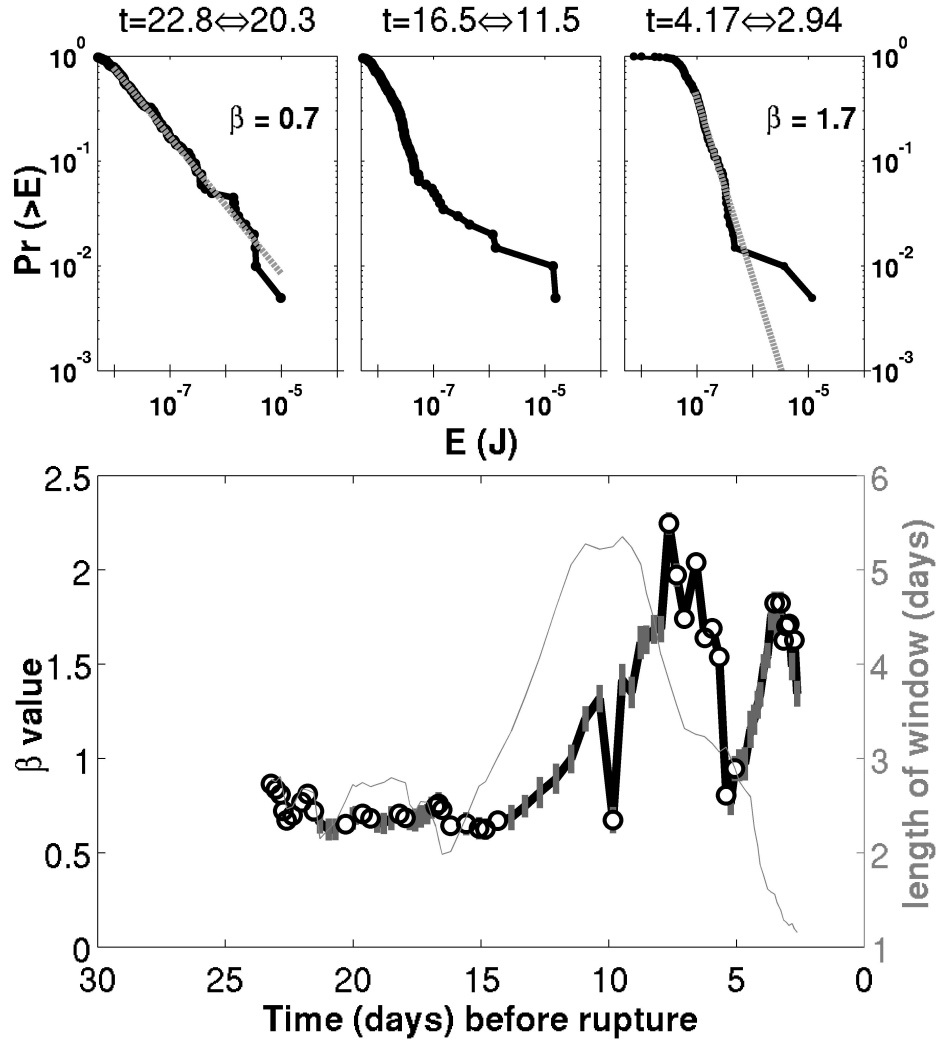


FIGURE 5. The three plots at the top show the complementary cumulative size-frequency distribution (CSFD) ($Pr(> E)$) of icequake energies (E) obtained in three windows of 200 events each, ending at the time indicated in the panels. The lower plot shows the evolution of the exponent β of the power law fitting the CSFD obtained in running windows of 200 events. The exponent β has been estimated using the Maximum Likelihood method (see text). The thin line also gives the duration of the sliding window of 200 events, corresponding to the scale on the right. The vertical lines indicate the errors given by the Maximum Likelihood method. Empty symbols indicate those fits whose p-value is greater than 0.2, i.e., for which the power-law behavior is plausible (see text).

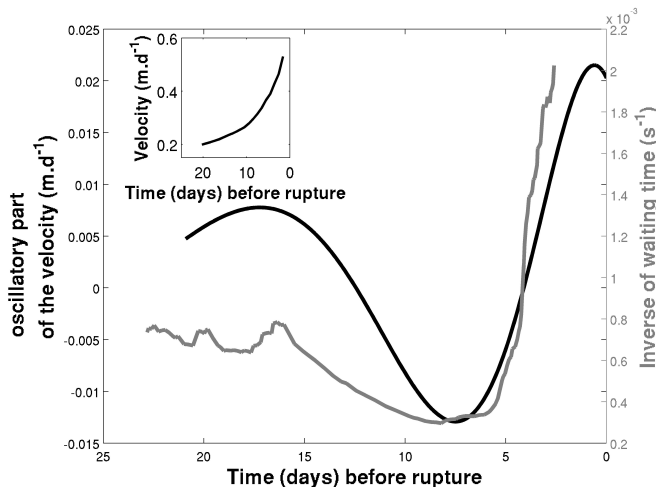


FIGURE 6. Plot of the inverse of the waiting time between successive icequakes (noisy grey curve) and of the oscillatory part of the evolution of the surface velocity (smooth dark oscillatory curve). Inset: surface velocity as a function of time up to the first break-off.

p-value was defined as being the fraction of the synthetic distances that were larger than the empirical distance. If p was not too small, the difference between the empirical and the synthetic data could be attributed to statistical fluctuations alone; if $p < 0.1; 0.05$, the fit was poor and the model was not appropriate at the 90%; 95% confidence level. By applying the p-test on our data, we obtained p-values greater than 0.2, indicated in Fig. 5 by empty symbols. This corresponds to the time windows for which we cannot reject the hypothesis that the CSFD was indeed generated from a power law distribution.

Three different behaviors were observed in succession:

- (i) For the windows located near the beginning of our measurements (up to $t = 14$ d), the CSFD was well described by a power-law distribution over at least 3 orders of magnitude (see upper left panel of Fig. 5), indicating a scale invariance of the acoustic emissions.
- (ii) From $t = 14$ d to $t = 8$ d, the exponent β exhibited a rapid shift, suggesting a change in behavior of the damage process developing in the ice mass. As the p-values were low in this period, the power-law behavior was not a plausible fit to the data.
- (iii) For the time windows near the end of our observation period (after $t = 8$ d), the CSFD recovered a power-law behavior, with a high β -value, with a shoulder at the tail of the distribution (upper right panel of Fig. 5).

4.3. Waiting time distribution and accelerating rate of icequakes. The time evolution of the rate of icequakes is well-captured by the inverse of the mean time lag between two consecutive icequakes. Fig. 6 shows this inverse mean time lag (which can be associated with a mean frequency of icequake events, i.e. the seismic activity) in a moving window containing 100 events as a function of the

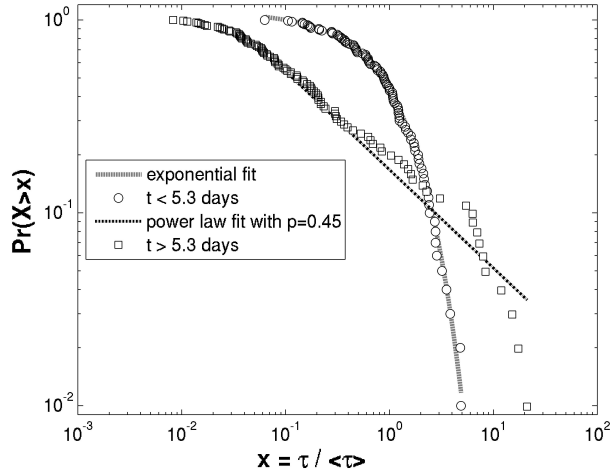


FIGURE 7. Complementary waiting time distribution ($Pr(X > x)$) for the 100 events before and after the transition ($\simeq 5.2$ days) between stable and unstable regimes. τ is the waiting time between two icequakes, $\langle \tau \rangle$ is the mean of all the waiting times considered. The data for $t \leq 5.2$ days can be well fitted by the exponential function $p(x) \sim a \cdot \exp(bx)$ with $a = 110$ and $b = -0.93$. For $t \geq 5.2$ days, the distribution of waiting times was compatible with a power law $p(x) \sim x^{-\alpha}$ for $x > x_{min}$ with $\alpha=1.5$ and $x_{min} = 0.058$.

time of the last point of the window. One can clearly observe a general acceleration of the icequake activity approximately one week before the break-off of the glacier. The size of the moving window was set as small as possible to enable an accurate practical detection of the acceleration of the icequake activity.

We performed the same statistical analysis as for icequake energy (see Section 4.2). Fig. 7, which shows the complementary cumulative size-frequency distribution of waiting time between two icequakes, exhibits a change in the waiting time distribution as the global rupture is approached. It appears that this distribution is initially well described by a power law distribution, indicating a temporal correlation between the icequakes. A few days before the glacier break-off, the waiting times distribution shifted to an exponential distribution, indicating a loss of temporal correlation between the icequakes.

4.4. Surface displacements. Thanks to very accurate displacement measurements ($< 1\text{cm}$), Faillettaz and others (2008) were able to demonstrate the existence of log-periodic oscillations superimposed on the power law acceleration. Log-periodicity, that is periodicity in the logarithm of the time-to-rupture $t_c - t$ (where the rupture occurs at time t_c), is the empirical signature of the symmetry of discrete scale invariance, which means that the observable is self-similar to itself only under integer powers of a fundamental scaling ratio λ of time scales (see review and details in Sornette (1998)).

This log-periodic behavior can be shown by the following equation describing the surface displacement as a function of time:

$$(4.1) \quad s(t) = s_0 + a(t_c - t)^m \left[1 + C \sin \left(2\pi \frac{\ln(t_c - t)}{\ln(\lambda)} + D \right) \right].$$

Here, s_0 is a constant, t_c is the critical time at which the global collapse is expected, $m < 1$ is the power law exponent quantifying the acceleration, a is a constant, C is the relative amplitude of the oscillations with respect to the overall power law acceleration, λ is the so-called “scaling ratio” associated with the log-periodicity of expression (4.1) and D is the phase of the log-periodic oscillation.

5. INTERPRETATIONS AND DISCUSSIONS

5.1. Size-frequency distributions of icequake energy. As described in Section 4.2, three different regimes can be identified during the maturation of the rupture event:

- (i) The size-frequency distribution of icequake energy exhibits a power-law behavior, indicating a scale invariance of the acoustic emissions, similar to that characterizing earthquakes. For earthquakes, the corresponding Gutenberg-Richter law describes one of the most ubiquitous statistical regularities observed (see for instance Pisarenko and Sornette (2003) and references therein). It reads

$$(5.1) \quad N(> E) \sim E^{-\beta},$$

where $N(> E)$ is the number of events with an energy greater than E and β is the Gutenberg-Richter exponent found empirically close to 2/3 for shallow earthquakes (depths < 70 km) in subduction and transform fault zones. Up to $t = 14$ d, the exponent β is found to be compatible with the earthquake value $\beta = 0.65 \pm 0.1$.

This behavior can be associated with a stable critical regime, in accordance with the critical behavior of rupture found in sufficiently heterogeneous media (Johansen and Sornette, 2000), similar to critical phase transitions (from diffuse damage to crack nucleation). As this non-equilibrium system exhibits a kind of dynamic criticality without tuning any control parameter, this regime could be associated with a self-organized critical (SOC) behavior. We refer to Jensen (1998), Turcotte (1999) and Sornette (2006) for introductions and detailed presentations of the concepts and models of self-organized criticality. The first stable regime fulfills the characteristics of SOC: (a) power-law distributions, such as those observed in this regime, (b) a constant driving stress, (c) a threshold dynamics and (d) a very large number of interacting local entities (here, the micro cracks). In other words, in a such regime, the glacier has time to adapt to the new state induced by the rupture maturation process.

- (ii) In this transitional regime, the glacier can no longer adapt itself to the changes induced by rupture maturation, and the CSFD of icequakes is no longer a power law. A main feature of the extreme tail is the large “characteristic events”, that can be interpreted as the nucleation of the incipient rupture.

- (iii) The size-frequency distribution of icequake energy exhibits a power-law behaviour with lower b-value and an appearance of characteristic events. Pisarenko and Sornette (2003) have associated a change in the exponent β with a change in the rupture process. They proposed the following explanation of these two regimes: First, large exponents β are found in the distribution of acoustic emission energies recorded for heterogeneous materials brought to rupture, for which damage occurs mainly in the form of weak shear zones and open cracks. In other words, large exponents β are mainly an indication of an open crack mode of damage. Second, when damage develops in the form of “dislocations” or mode II cracks, with slip mode of failure and with healing, the exponent β is found to be smaller than 1.

This suggests that the low value of $\beta \simeq 2/3$ found up to two weeks before rupture is associated with a stable, slow and diffuse “dislocation-like” damage process. In the subsequent days, the increase in the exponent β , together with the developing shoulder at high icequake energies, can then be interpreted as revealing a transition to a mode of damage controlled more and more by crack openings and their coalescence prior to the incipient rupture.

The tail of the distribution develops a strong shoulder, indicating a change in the damage evolution process. The clear deficit of icequakes with low energies and the excess of large “characteristic” events (events with high energy) is fully compatible with the evolution of the second regime dominated by crack-like events which, by their proliferation and fusion, progressively nucleate the formation of the run-away macro-crack responsible for the final avalanche associated with a rather clean crack-like rupture, as shown in Fig. 1. Moreover, as coupling between cracks increases, and heterogeneity decreases, the power law develops a shoulder, corresponding to a different regime of global rupture (Sornette, 2009).

5.2. Seismic activity. Acoustic emissions were also observed experimentally in heterogeneous materials brought to rupture and were found to exhibit clear acceleration, in agreement with a power-law divergence expected from the critical point theory (Johansen and Sornette, 2000). In a nutshell, critical point theory views the global rupture of a system as the result of a progressive organization process of defects. The global rupture corresponds to a ‘bifurcation’ (also known as ‘phase transition’, ‘catastrophe’ or ‘tipping point’), resulting from the collective organization of defects that interact to prepare the global transition, i.e., the rupture (Sornette and Sornette, 1990; Sornette and Vanneste, 1990; Anifrani and others, 1995; Andersen and others, 1997; Sornette and Andersen, 1998; Sammis and Sornette, 2002). The concept of critical rupture suggests that global ruptures are preceded by specific precursors that make them predictable in a probabilistic way (Anifrani and others, 1995; Sornette, 2002).

Our results also support this picture as they clearly indicate a general acceleration in icequake activity approximately one week before the break-off event. Recent studies in material sciences also show a clear transition to the tertiary creep regime with an acceleration in the rate of acoustic emissions (Nechad and others, 2005a,b, and references therein).

5.3. Comparison between icequake activity and surface displacements.

Faillettaz and others (2008) demonstrated a general power-law acceleration of the surface displacement before the break-off of this hanging glacier. Moreover, this acceleration was accompanied by oscillations which increased logarithmically in frequency as the time of failure approached (referred to as log-periodic oscillations). The origin of such oscillations is not yet fully understood, but dynamic crack interactions were hypothesized as a possible mechanism leading to such log-periodic oscillations (Saleur and others, 1996; Huang and others, 1997; Ide and Andersen, 2002).

The discrete hierarchy of the organization of damage revealed by the log-periodic oscillations (Faillettaz and others, 2008) should somehow influence the seismic activity of the glacier during the maturation of the rupture process. Fig. 6 shows the comparison between the oscillatory part of the velocity (time derivative of the surface displacements which follow a log-periodic power law) and the inverse of the waiting time between successive icequakes.

It appears that these two metrics exhibit a significant correlation (with $r^2 = 0.65$). This result means that the seismic activity is not correlated with the global power-law acceleration of the glacier during the rupture maturation but rather with its superimposed oscillations. It is more the jerky motions around the overall accelerations that are responsible for detectable seismic activity (Johansen and Sornette, 1999), corresponding to crack growth and coalescence events within the glacier.

5.4. Waiting time distribution. The waiting time distribution was seen to be first power law distributed, and then it shifted to an exponential distribution. This result is in accordance with the previous physical interpretation of crack coalescence. We tentatively attribute this change of the distribution of waiting times from power-law to exponential to the transition from diffuse damage to damage organizing in the form of clusters.

The random activation of different damage clusters when approaching the global failure causes a transient loss of the temporal correlation of the individual fracture events (Kuksenko and others, 2005). This effect confirms the existence of a hierarchical structure of the fracture process in the glacier.

In contrast to the difficulties in ascertaining the existence of an accelerating moment release upon the approach to a large earthquake (Hardebeck and others, 2008), the four metrics that we applied to our glacier data support the existence in this case of an accelerated deformation and damage process occurring in the last few days before the incipient break-off.

5.5. Evolution of failure processes leading to the break-off event. It is now possible to draw the following picture of the evolution of the failure processes leading to the break-off event.

- (i) **From the beginning of our measurements to 15 days before the break-off event:** In this regime, seismic activity is more or less constant, the size-frequency distribution of icequake energies is described by a power-law behavior and the waiting time distribution is also a power law. This behavior could be related to a self-organizing regime, where diffuse damage accumulates within the glacier, with a proliferation of dislocation-like

defects. In other words, the glacier has time to adapt to the deformation and damage maturation process.

- (ii) **From 15 days to 5 days before the break-off event:** seismic activity is slightly decaying, the size-frequency distribution is no longer power-law, the waiting time distribution is power law and the glacier is decelerating relative to the previous phase. This is a transitional regime: the damage process goes on, micro-cracks grow and start merging in a homogeneous way. Log-periodic oscillations appear and reveal the hierarchical structure of the fracture process under development. In such a regime, screening and locking effects are likely to appear, possibly explaining the slight decay of icequake activity and the relative slowdown of surface velocity.
- (iii) **From 5 days before the final break-off event:** Seismic activity drastically increases, the size-frequency distribution of icequake energy recovers its power-law behavior but with a different exponent, together with the appearance of some large characteristic events leading to a strong shoulder in the distribution. The waiting time distribution exhibits a shift from a power law to an exponential distribution. The system enters into a catastrophic regime where damage clusters are randomly activated. Damage clusters interact and merge with a preferential direction (i.e. preparing the final rupture pattern), in contrast to the previous regime. The largest scale of the hierarchical structure of the fracture process is activated (resulting in characteristic events).

6. SUMMARY AND PERSPECTIVES

We have presented and studied a unique data set of icequakes recorded in the immediate vicinity of a hanging glacier over 25 days prior to and up to its rupture. While seismic measurement records unfortunately ceased 3 days before the first break-off and 10 days before the larger subsequent one, we nevertheless were able to obtain a coherent quantitative picture of the damage process developing before the impending glacier collapse. Our main results include first the demonstration of a clear increase in the icequake activity within the glacier (measured as the inverse of the waiting time between successive icequakes) starting approximately 6 days before the first break-off. Secondly, we found a two-step evolution of the size-frequency distribution of icequake energies, characterizing a first transition to a crack-like dominated damage followed by a second transition in which large characteristic cracks prepared the nucleation of the run-away rupture. Thirdly, we documented the acceleration of the rate of icequakes combined with a change in the distribution of waiting times between icequakes, which is typical for the hierarchical cascade of rupture instabilities found in earlier reports on the acoustic emissions associated with the failure of heterogeneous materials. Moreover, a clear correlation between the seismic activity and the oscillatory part of the surface velocity evolution prior to the first break off event was also documented. By combining the analysis of surface motion with log-periodic oscillations and icequake activity during the rupture maturation process, prediction of the final break-off time was improved significantly. This also provides new insights into the physical mechanisms of the rupture in heterogeneous materials.

Provided that technical solutions can be found to ensure continuous icequake recordings in the difficult high-altitude mountain conditions, our results clear the

path for real-time diagnostics of impending glacier failure. The next steps towards this goal include (a) developing an automatic seismic data processing in real time (which includes the automatic detection of icequakes and the determination of their energy), (b) processing these data with the statistical tools developed here, and (c) performing systematic reliability tests to access the rate of false alarms (false positives or errors of type I) versus missed events (false negatives or errors of type II). Step (c) is necessary for an informed cost-benefit analysis of the societal and economic impacts of the proposed real-time forecast methodology.

Acknowledgements: The Institute of Geophysics at the ETH Zürich is gratefully acknowledged for allowing us the use of their instruments. Thanks are extended to Dr. Fabian Walter for fruitful discussions. Dr. Paul Winberry, as well as an anonymous referee and Ted Scambos contributed substantially to the improvements made in the manuscript. We are also grateful to C. Wuilloud (natural hazards, Valais) for logistic and financial support.

REFERENCES

- Allen, R. V. 1978. Automatic earthquake recognition and timing from single traces. *B. Seismol. Soc. Am.*, **68**, (5), 1521-1532.
- Amitrano, D., J.-R. Grasso and G. Senfaute. 2005. Seismic precursory patterns before a cliff collapse and critical point phenomena, *Geophys. Res. Lett.*, **32**:L08314.
- Andersen, J.V., D. Sornette and K.-T. Leung. 1997. Tri-critical behavior in rupture induced by disorder, *Phys. Rev. Lett.*, **78**, 2140-2143.
- Anifrani, J.-C., C. Le Floch, D. Sornette and B. Souillard. 1995. Universal Log-periodic correction to renormalization group scaling for rupture stress prediction from acoustic emissions, *J. Phys. I France*, **5**, 631-638.
- Clauset A., C. Rohilla Shalizi and M. E. J. Newman. 2009. Power law distributions in empirical data, *SIAM Review* 51, 661-703.
- Deichmann, N., J. Ansorge, F. Scherbaum, A. Aschwanden, F. Bernhardt and G. H. Gudmundsson. 2000. Evidence for deep icequakes in an Alpine glacier, *Ann. Glaciol.*, **31**, 85-90.
- Dixon, N., R. Hill and J. Kavanagh. 2003. Acoustic emission monitoring of slope instability: development of an active waveguide system, *Geotechnical Engineering*, **156**, 83-95.
- Dixon, N. and M. Spriggs. 2007. Quantification of slope displacement rates using acoustic emission monitoring, *Can. Geotech. J.*, **44**, 966-976.
- Ekstrom, G., M. Nettles and G. Abers. 2003. Glacial earthquakes. *Science*, **302**, 622.
- Ekstrom, G., M. Nettles and V. Tsai. 2006. Seasonality and increasing frequency of greenland glacial earthquakes. *Science*, **311**, 1756.
- Faillottaz, J., A. Pralong, M. Funk and N. Deichmann. 2008. Evidence of log-periodic oscillations and increasing icequake activity during the breaking-off of large ice masses. *J. Glaciol.*, **57**, (187), 725.
- Flotron, A. 1977. Movement studies on hanging glaciers in relation with an ice avalanche, *J. Glaciol.*, **19** (81), 671-672.
- Hardebeck, J. L., K. R. Felzer and A. J. Michael. 2008. Improved tests reveal that the accelerating moment release hypothesis is statistically insignificant. *J. Geophys. Res.*, **113** (B8), B08310.

- Huang, Y., G. Ouillon, H. Saleur and D. Sornette. 1997. Spontaneous generation of discrete scale invariance in growth models, *Phys. Rev. E*, **55** (6), 6433-6447.
- Ide K. and D. Sornette. 2002. Oscillatory Finite-Time Singularities in Finance, Population and Rupture, *Physica A*, **307** (1-2), 63-106.
- Jensen, H. J. 1998. Self-Organized Criticality (Cambridge: Cambridge University Press).
- Johansen, A. and D. Sornette. 1999. Acoustic radiation controls friction: evidence from a spring-block experiment, *Phys. Rev. Lett.*, **82**, (25), 5152-5155.
- Johansen, A. and D. Sornette. 2000. Critical ruptures. *Eur. Phys. J. B*, **18**, 163.
- Kolesnikov, Yu. I., M. M. Nemirovich-Danchenko, S. V. Goldin and V. S. Seleznev. 2003. Slope stability monitoring from microseismic field using polarization methodology. *Nat. Haz. Earth Sys. Sc.*, **3**, 515-521.
- Kuksenko, V., N. Tomilin and A. Chmel. 2005. The role of driving rate in scaling characteristics of rock fracture. *J. Stat. Mech.*, P06012.
- Lüthi, M., 2003. Instability in glacial systems, *Milestones in Physical Glaciology: From pioneers to a Modern Science. Mitteilungen, VAW/ETHZ*, **180**, 63-70.
- MacAyeal, D.R., E.A. Okal, R.C. Aster and J.N. Bassis. 2008. Seismic and hydroacoustic tremor generated by colliding icebergs, *J. Geophys. Res.*, **113**, F03011, doi: 10.1029/2008JF001005.
- Neave, K. G. and J. C. Savage. 1970. Icequakes at Athabasca Glacier. *J. Glaciol.*, **49**, 587-598.
- Nechad, H., A. Helmstetter, R. El Guerjouma and D. Sornette. 2005. Andrade and Critical Time-to-Failure Laws in Fiber-Matrix Composites: Experiments and Model, *J. Mech. Phys. Solids*, **53**, 1099-1127.
- Nechad, H., A. Helmstetter, R. El Guerjouma and D. Sornette. 2005. Creep rupture in heterogeneous materials, *Phys. Rev. Lett.*, **94**, 045501.
- O'Neel, S., H. P. Marshall, D.E. McNamara and W. T. Pfeffer. 2007. Seismic detection and analysis of icequakes at Columbia Glacier, Alaska. *J. Geophys. Res.*, **112**, F03S23.
- Neetles, M. and 12 others. 2008. Step-wise changes in glacier flow speed coincide with calving and glacial earthquakes at Helheim Glacier, Greenland, *Geophys. Res. Lett.*, **35**, L24503, doi: 10.1029/2008GL036127.
- Pisarenko, V.F. and D. Sornette. 2003. Characterization of the frequency of extreme earthquake events by generalized the Pareto distribution, *Pure Appl. Geophys.*, **160**, 2343-2364.
- Pralong, A. and M. Funk. 2006. On the instability of avalanching glaciers, *J. Glaciol.*, **52** (176), 31-48.
- Pralong, A., C. Birrer, W. Stahel and M. Funk. 2005. On the Predictability of Ice Avalanches, *Nonlin. Processes Geophys.*, **12**, 849-861.
- Raymond, M., M. Wegmann and M. Funk. 2003. Inventar gefährlicher Gletscher in der Schweiz, *Mitteilung, VAW, ETHZ*, 182.
- Röthlisberger, H. 1981. Eislawinen und Ausbrüche von Gletscherseen, in P. Kasser (Ed.), *Gletscher und Klima - glaciers et climat*, Jahrbuch der Schweizerischen Naturforschenden Gesellschaft, wissenschaftlicher Teil 1978, pp 170-212, Birkhäuser Verlag Basel, Boston, Stuttgart.
- Roux, P.-F., D. Marsan, J-P. Metaxian, G. O'Brien and L. Moreau. 2008. Microseismic activity within a serac zone in an alpine glacier (Glacier d'Argentière, Mont-Blanc, France). *J. Glaciol.*, **54**, (184), 157.

- Saleur, H., C.G. Sammis and D. Sornette, 1996. Discrete scale invariance, complex fractal dimensions and log-periodic corrections in earthquakes, *J. Geophys. Res.*, **101**, NB8, 17661-17677.
- Sammis, S.G. and D. Sornette. 2002. Positive Feedback, Memory and the Predictability of Earthquakes, *Proc. Natl. Acad. Sci. USA*, **99**, SUPP1, 2501-2508.
- Sornette, D. 1998. Discrete scale invariance and complex dimensions, *Phys. Rep.*, **297** (5), 239-270.
- Sornette, D. 2002. Predictability of catastrophic events: material rupture, earthquakes, turbulence, financial crashes and human birth, *Proc. Natl. Acad. Sci. USA*, **99**, SUPP1, 2522-2529.
- Sornette, D. 2006. Critical Phenomena in Natural Sciences (Chaos, Fractals, Self-organization and Disorder: Concepts and Tools), 2nd ed., pp.528, 102 figs. , 4 tabs (Springer Series in Synergetics, Heidelberg).
- Sornette D. 2009. Dragon-Kings, Black Swans and the prediction of Crises, *Int. J. Terraspace Sc. Eng.*, **2** (1), 1-18.
- Sornette, D. and J. V. Andersen. 1998. Scaling with respect to disorder in time-to-failure, *Eur. Phys. Journal B*, **1**, 353-357.
- Sornette, A. and D. Sornette. 1990. Earthquake rupture as a critical point: Consequences for telluric precursors, *Tectonophys.*, **179**, 327-334.
- Sornette, D. and C.Vanneste. 1990. Dynamics and memory effects in rupture of thermal fuse networks, *Phys. Rev. Lett.*, **68**, 612-615.
- St. Lawrence W. and A. Qamar. 1979. Hydraulic Transients: A Seismic Source in Volcanoes and Glaciers *Science*, New Series, **203**, 4381 (Feb. 16, 1979), 654-656.
- Tsai, V. C., J. R. Rice and M. Fahnestock. 2008. Possible mechanisms for glacial earthquakes. *Journal of Geophysical Research*, **113**, F03014, doi:10.1029/2007JF000944.
- Turcotte, D. L. 1999. Self-organized criticality, *Rep. Prog. Phys.*, **62**, 1377-1429.
- Walter, F., N. Deichmann and M. Funk. 2008. Basal icequakes during changing subglacial water pressures beneath Gornergletscher, Switzerland. *J. Glaciol.*, **54**, (186), 511.
- Weaver, C. and S. Malone. 1979. Seismic evidence for discrete glacier motion at the rock-ice interface. *J. Glaciol.*, **23**, (89), 171.

J. FAILLETTAZ, VAW, ETH ZURICH, LABORATORY OF HYDRAULICS, HYDROLOGY AND GLACIOLOGY, SWITZERLAND

E-mail address: faillettaz@vaw.baug.ethz.ch

DD. SORNETTE, EPARTMENT OF MANAGEMENT, TECHNOLOGY AND ECONOMICS, ETH ZÜRICH

DEPARTMENT OF EARTH SCIENCES, ETH ZÜRICH

INSTITUTE OF GEOPHYSICS AND PLANETARY PHYSICS, UCLA

Current address: Department of Management, Technology and Economics,, ETH Zürich, Switzerland

E-mail address: dsornette@ethz.ch

M. FUNK, VAW, ETH ZURICH, LABORATORY OF HYDRAULICS, HYDROLOGY AND GLACIOLOGY, SWITZERLAND

E-mail address: funk@vaw.baug.ethz.ch